sustainability

MDPI

Article

Comprehensive Utilization and Sustainable Development of Bauxite in Northern Guizhou on a Background of Carbon Neutralization

Wu Yang [1,2], Min Zhang [1,2,*], Cui Tao [1,2] and Jun Yan [1,2]

[1] Faculty of Resources and Environmental Engineering, Guizhou Institute of Technology, Guiyang 550003, China
[2] Engineering Research Center of Carbon Neutrality in Karst Areas, Ministry of Education, Guiyang 550003, China
* Correspondence: zhangmin@git.edu.cn

Abstract: As a developing country, China is also a major producer and consumer of mineral resources. At present, China is still in a critical period of rapid development of industrialization and urbanization, which will inevitably lead to huge resource consumption. It is only 30 years between the peak carbon consumption and the timepoint planned to achieve the goal of carbon neutrality. Coming from a background of dual pressure in terms of the total amount and intensity of "carbon neutrality", the development and utilization of mineral resources has become one of the important factors in affecting and realizing carbon neutrality in China, and comprehensive utilization has become increasingly important. There are abundant bauxite resources in northern Guizhou, more than 700 million tons, and an industrial resource chain could be built around bauxite. The ore-forming process of bauxite is very complex, and there are enrichment phenomena of other useful elements in the ore-bearing rock series, among which the enrichment of associated Ga, Li and rare earth elements is very obvious. It is of great economic and scientific significance to study the migration law of associated Ga, Li and rare earth elements and to find out whether these elements in bauxite have development value. On the basis of systematically collecting and sorting previous research results, this study carried out supplementary tests on some areas with insufficient data; summarized and studied the migration law of associated Ga, Li and rare earth elements in the Wuzhengdao bauxite deposit in northern Guizhou; and conducted a feasibility analysis on the development and utilization prospects of associated Ga, Li and rare earth elements.

Keywords: carbon neutral; Guizhou; bauxite; comprehensive utilization; statistical analysis

check for updates

Citation: Yang, W.; Zhang, M.; Tao, C.; Yan, J. Comprehensive Utilization and Sustainable Development of Bauxite in Northern Guizhou on a Background of Carbon Neutralization. *Sustainability* **2022**, *14*, 14301. https://doi.org/10.3390/su142114301

Academic Editor: Marco Lezzerini

Received: 18 September 2022
Accepted: 29 October 2022
Published: 1 November 2022

Publisher's Note: MDPI stays neutral with regard to jurisdictional claims in published maps and institutional affiliations.

Copyright: © 2022 by the authors. Licensee MDPI, Basel, Switzerland. This article is an open access article distributed under the terms and conditions of the Creative Commons Attribution (CC BY) license (https://creativecommons.org/licenses/by/4.0/).

1. Introduction

Bauxite is a strategic mineral resource and the most important raw material for the extraction of metallic aluminum [1–4]. China's bauxite is mainly distributed in Shanxi, Guangxi, Henan and Guizhou. The bauxite in Guizhou is mainly from the central and northern areas. Many experts and scholars have conducted long-term research on the bauxite in northern Guizhou and achieved fruitful results, which are mainly manifested in the petrology and mineralogy of the bauxite and the characteristics of the deposit; the sedimentary environment and sedimentary facies; and the geochemical characteristics [5–10]. Based on the mineral geochemical characteristics and spatial variation in the bauxite deposit, the provenance of the bauxite was identified and traced, and the metallogenic mechanism and mineralization were analyzed. The Wuzhengdao bauxite deposit in northern Guizhou is of great value for development and utilization, as the associated Ga, Li and rare earth elements are enriched and there is potential for comprehensive or independent development and utilization. Studying the migration and enrichment of associated elements is not only a very meaningful scientific issue, but can also greatly improve the value of bauxite, provide

rare metal resources for national development and promote local economic development. In this context, the project studied the migration law of associated Ga, Li and rare earth elements in bauxite and the key controlling factors of mineralization, as well as analyzed its development and utilization prospects.

2. Materials and Methods

In this study, we mainly used two methods: (1) the literature method, using the published articles in the region to summarize the public data; (2) supplementary testing for the lack of data in the region, via supplemental sampling test analysis, to strive to make the whole study more comprehensive. On this basis, the research was carried out under the guidance of the resource endowment theory, the "two mountains" theory and the "two common" theory put forward by General Secretary Xi, with carbon neutralization and mineral resources at the center, and combined with the seven-year practical experience of the research team of the Guizhou Institute of Technology [11–15].

2.1. The Literature Method

Using the document information retrieval tool, we searched the Web of Science, Engineering Index, CNKI and Google and collected 134 pieces of basic data related to the comprehensive utilization of bauxite in Guizhou, which were subdivided according to the following three categories:

(1) Comprehensive study of the geological characteristics, development horizon and distribution law of associated mineral resources in Guizhou.

Associated element minerals in Guizhou are characterized by multiple metallogenic epochs, diverse metallogenic environments and complex metallogenic mechanisms, which can be roughly divided into three genetic types: sedimentary, hydrothermal and magmatic. This included fully collecting and analyzing the regional basic geological and integrated exploration data; implementing some drilling projects; exploring the development horizon, distribution, depth and thickness changes in associated minerals; studying their rock types, geochemical characteristics and occurrence states; dividing the enrichment strata of associated elements according to the geological–geochemical characteristics of ore-bearing rocks; and summarizing the space–time distribution law of associated minerals.

(2) Evaluation of associated mineral resources and optimization of prospecting targets in Guizhou.

This included selecting and determining the resource evaluation methods suitable for the geological characteristics and conditions of the associated minerals in Guizhou, obtaining the industrial index system of associated mineral resource evaluation, determining the key characteristic parameters, summarizing the metallogenic geological conditions and enrichment laws of associated minerals, evaluating the potential of associated mineral resources and delineating favorable prospecting targets.

(3) Establishing a pilot project of comprehensive investigation, evaluation and re-use technology of associated mineral tailings resources in Guizhou.

At present, it is urgent to study the comprehensive evaluation and re-use of associated mineral resources in bauxite (tailings). Tailings reservoirs are scattered all over the province, which not only occupy a large amount of land resources, but also cause serious hidden dangers in terms of environmental protection, which does not meet the requirements of modern social development for the construction of ecological civilization. Therefore, it is necessary to locate tailings resources as soon as possible, and to carry out feasibility studies on the rational utilization technology of associated elemental minerals to provide a basis for the special formulation of their development and utilization technology programs.

2.2. Supplementary Test

For research gaps that were missing in the extant literature, we conducted a supplemental sampling test analysis. The samples of this work were collected from Permian bauxite in northern Guizhou, including 12 pieces of clastic bauxite, 18 pieces of dense massive bauxite and 14 pieces of ferruginous claystone (Figure 1).

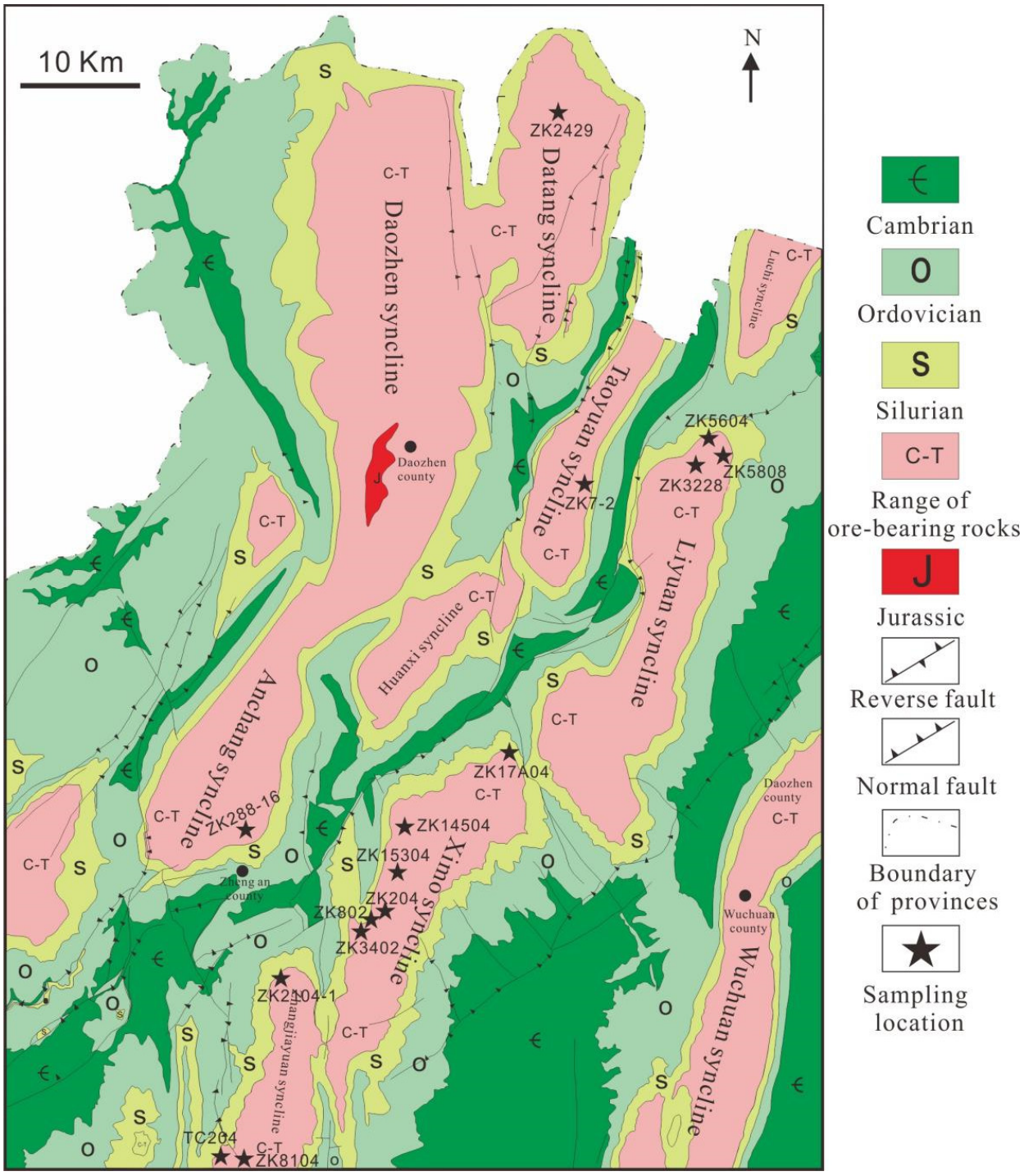


Figure 1. Geologic map of WZD area in northern Guizhou (Cui, 2021 [1]).

The samples were analyzed by the State Key of Geological Processes and Mineral Resources of the China University of Geosciences (Wuhan, China) Laboratory and Guangzhou Aoshi Analysis and Testing Co., Ltd.

The main elements were analyzed using the X-ray fluorescence spectrometer melting method, and the specific steps were as follows: Samples were crushed and ground to less than 200 mesh, and two samples were taken. A lithium borate–lithium nitrate melting flux containing lithium nitrate was added to one sample and melted at high temperature after full mixing. The molten material was poured into a platinum mold to form a flat glass sheet, and then analyzed using an X-ray fluorescence spectrometer. At the same time, the other sample was burned in a Muffle furnace at 1000 °C, cooled and weighed. The weight difference between the sample before and after heating was the firing loss. In the process of the principal element analysis, GBW07105, NCSDC009, SA RM-4, SARM-5, GBW07104 and GBW07108 were the reference materials, and the error was less than 5%.

Trace elements were analyzed by inductively coupled plasma emission spectroscopy and mass spectrometry. The specific steps were as follows: Samples were crushed and ground to less than 200 mesh, and two samples were weighed. One sample was digested with perchloric acid, nitric acid and hydrofluoric acid. After steaming to near drying, the samples were dissolved in dilute hydrochloric acid and then analyzed by plasma emission spectroscopy and plasma mass spectrometry. The other sample was added to a lithium metaborate/lithium tetraborate flux, mixed evenly and melted in a furnace above 1025 °C. After cooling, the molten liquid was fixed with nitric acid, hydrochloric acid and hydrofluoric acid, and then used for isoseparation and a daughter ion mass spectrometry analysis. In the process of the trace element analysis, GBM908-10, MRGeo08, OreAS-120 and Stsd-1 were used as the reference materials, and the error of other elements was <7%, except for some elements.

An X-ray powder diffraction analysis was carried out by the China University of Geosciences (Wuhan, China), Geological Processes and Mineralization National Center Point Lab. The testing equipment and conditions were as follows: Panaco X 'Pert Pro X X-ray powder diffractometer, with a working voltage of 40 kV, working current of 40 ma, Cu target, Ni filter, continuous scanning, step 0. 017° and step 5S/step. Eight samples were selected for the clay separation test. According to the directional XRD analysis of the purified clay, the main clay mineral types were obtained, and the natural sheet, ethylene glycol saturated sheet and heating 550 °C stage test were used. The clay minerals were determined by an XRD analysis.

The lithium non-roasting mixed-acid leaching experiment was completed at the Mining College of Guizhou University. The aluminous rock in central Guizhou used in this experimental study was treated by crushing, reduction, grinding and screening to obtain samples with an appropriate particle size. The mixed acid was prepared by uniformly mixing sulfuric acid and phosphoric acid in deionized water. The samples were analyzed by X-ray fluorescence spectrometry. The mineralogical composition of the ore and post-extraction residue was determined using a copper target equipped with an X-ray diffractometer analysis in the 2 theta range of 5–75 deg. The concentration of aluminum and lithium elements leached into the solution was determined by inductively coupled plasma spectrometry (ICP-AES) [16–20].

3. Results

3.1. Data Collection from the Literature

By reading and sorting out data from more than 100 articles, we found that the bauxite deposits in Guizhou are generally rich in gallium, which is determined by the similar outer electronic shell structure of gallium and aluminum. It has been found that gallium is dispersed in aluminum minerals and aluminum-bearing clay minerals, and mainly exists in diaspore; the worse the crystallization degree of diaspore, the higher the content of gallium. Gallium content in ore-bearing rock series and ores in different ore belts is related to gallium content in the rocks of basement strata, but generally, gallium will be gradually enriched with the increase in Al_2O_3 content in bauxite, and the cumulative amount of associated gallium ore in the bauxite of the whole province is more than 30,000 t (Tables 1–3).

Table 1. Content of associated elements in Guizhou bauxite (10^{-6}).

Ore Field Division	Serial Number	County/City	Name	Companion Minerals	Grade of Associated Elements	Al_2O_3 (%)	Associated Resources (t)	Bauxite Resources (10,000 t)
Guiyang-Qingzhen bauxite ore field	1	Xiuwen County	Xiaoshan Dam	Ga,Sc, Ge	0.0031~0.005; 0.00287~0.00752; 0.000243~0.000547	68.47	Ga:666	1343
	2	Xiuwen County	Arrow shaft punch	Ga	0.0022~0.0136	65.36	220.59	407
	3	Xiuwen County	Dry Dam	Ga,Sc	Ga:0.006	63.52	Ga:777	646
	4	Xiuwen County	Changchong	Ga,Sc	Ga:0.005	63.4	Ga:388	786
	5	Qingzhen city	Cat Farm	Ga,Ge,Sc	0.0058; 0.001~0.1; 0.065	67.6	Ga:9317	178508
	6	Qingzhen city	Lin Dao	Ga,Sc,Zr	0.0067; 0.0023~0.0072; 0.01	66.32	Ga:543	689
	7	Qingzhen city	Yan Long	Ga	0.0073	70.85	558.59	680
	8	Qingzhen city	Mai Ba	Ga	0.0087	65.68	1006	1255
	9	Qingzhen city	Meg	Ga, Sc	0.0061; 0.00287~0.00752	67.49	Ga:276	600
	10	Guiyang City	Cape Hill	Ga	0.0094	66.05	1081.54	817
Zunyi-Xifeng bauxite ore field	11	Zunyi County	Rear Slot	Ga.V	0.0132; 0.0139~0.0674	67.04	Ga:1594	993
	12	Zunyi County	Chuanzhu Temple	Ga	0.0134	65.65	818	544
	13	Zunyi County	New Station	Ga	0.012	60.22	-	331
	14	Zunyi County	Gou Jiang	Ga	0.014	65.22	905	678
	15	Zunyi County	Song Jia Dalin	Ga	0.0109	63.5	743.95	513
	16	Zunyi County	Fairy Rock	Ga	0.0098	57.45	1499	-
	17	Kaiyang County	Zhao Jiawan	Ga	0.0157	61.43	-	428.5
	18	Kaiyang County	Xinzhai	Ga	0.0155	70.47	-	-
	19	Xifeng County	Shuitou village	Ga	0.0135	62.26	-	-

Table 1. *Cont.*

Ore Field Division	Serial Number	County/City	Name	Companion Minerals	Grade of Associated Elements	Al_2O_3 (%)	Associated Resources (t)	Bauxite Resources (10,000 t)
Wuchuan-Zhengan-Daozhen bauxite ore field	20	Daozhen, Wuchuan, Xinmin, Zhengan County	Dazhuyuan	Ga,W,Li,Zr	0.0086; 0.1~0.22; Li_2O:0.0984; 0.0818	68.85	Ga:5448.25 Li_2O: 62337.97	3564
	21	Wuchuan County	Wachangping	Ga.Li	Ga:0.01~0.03; Li_2O_5:0.1-0.5	73	Ga:7372; Li_2O_5:69188	4397

Table 2. Analysis results of main elements of bauxite.

Sample	Deep (m)	Na_2O	MgO	Al_2O_3	SiO_2	P_2O_5	K_2O	CaO	TiO_2	MnO	Fe_2O_3	LOI	Total
ZK14904-4	386.7	0.54	1.96	30.05	39.08	0.04	3.79	0.27	2.12	0.01	8.11	13.89	99.86
ZK14904-5	387.0	0.43	2.40	31.02	36.59	0.07	2.06	0.15	1.77	0.02	10.69	14.73	99.93
ZK14904-7	387.9	0.03	1.93	54.65	7.89	0.05	0.01	0.26	4.22	0.05	15.42	15.38	99.89
ZK14904-8	388.1	0.04	1.81	58.57	8.22	0.09	0.05	0.35	5.24	0.05	11.74	13.73	99.89
ZK14904-9	388.6	0.02	1.61	61.13	7.96	0.10	0.01	0.01	3.20	0.03	12.44	13.38	99.89
ZK14904-10	389.0	0.06	2.00	56.75	9.95	0.09	0.01	0.01	2.71	0.04	15.43	12.86	99.91
ZK14904-13	390.5	0.05	0.66	67.31	3.55	0.10	0.01	0.09	3.34	0.02	6.52	18.31	99.96
ZK14904-14	390.9	0.04	0.92	60.59	5.58	0.07	0.01	0.01	2.75	0.02	10.61	19.35	99.95
ZK14904-15	391.6	0.04	1.24	54.81	7.7	0.12	0.01	0.01	3.99	0.03	14.57	17.41	99.93
ZK14904-16	392.1	0.04	1.20	53.65	7.93	0.07	0.01	0.01	3.41	0.02	15.11	18.47	99.92
ZK14904-17	393.2	0.04	1.38	57.40	7.77	0.07	0.01	0.01	3.05	0.02	13.67	16.50	99.92
ZK14904-19	393.4	0.06	2.54	45.80	13.53	0.10	0.01	0.01	2.51	0.04	21.45	13.89	99.94
ZK14904-20	393.5	0.04	3.55	36.82	18.38	0.09	0.01	0.01	2.01	0.04	27.67	11.29	99.91
ZK14904-21	394.1	0.13	3.94	32.07	34.35	0.08	0.44	0.05	1.55	0.03	14.94	12.35	99.93
ZK14904-22	395.3	0.22	3.47	30.47	34.13	0.10	1.14	0.07	1.52	0.03	17.95	10.77	99.87
ZK14904-23	396.5	0.22	3.10	30.36	33.58	0.08	1.23	0.08	1.63	0.03	19.27	10.35	99.93
ZK14904-24	397.6	0.30	2.30	32.03	36.95	0.08	1.78	0.07	1.76	0.02	14.15	10.55	99.99
ZK14904-25	398.3	0.31	2.53	30.60	35.13	0.06	1.69	0.11	1.71	0.03	17.63	10.11	99.91
ZK14904-26	398.8	0.03	1.32	62.33	6.83	0.12	0.01	0.05	3.38	0.03	11.33	14.47	99.90
ZK14904-27	399.6	0.13	3.63	33.83	37.99	0.05	0.18	0.08	2.39	0.01	8.24	13.42	99.95
ZK702-2	199.6	0.04	0.87	75.16	4.04	0.05	0.02	0.01	4.44	0.01	0.77	14.53	99.94
ZK702-3	201.7	0.07	0.69	38.69	42.07	0.04	0.16	0.10	1.70	0.01	1.83	14.55	99.91
ZK702-4	202.3	0.19	0.51	36.56	42.8	0.04	0.38	0.12	1.63	0.01	3.16	14.56	99.96
ZK702-5	203.5	0.08	3.47	32.25	34.05	0.04	0.07	0.07	1.79	0.14	16.00	11.99	99.95
ZK702-6	204.8	0.59	1.38	35.17	41.85	0.08	1.73	0.12	1.46	0.04	5.78	11.76	99.96
ZK3402-3	297.7	0.19	4.22	40.33	31.88	0.05	1.62	0.08	3.00	0.01	4.52	14.00	99.90
ZK3402-4	298.3	0.08	4.95	40.27	23.75	0.06	0.38	0.06	2.07	0.01	12.42	15.90	99.95
ZK3402-6	299.6	0.03	1.12	72.27	4.49	0.12	0.04	0.01	3.05	0.01	4.22	14.55	99.91
ZK3402-7	299.8	0.03	1.13	71.50	4.52	0.06	0.03	0.01	3.73	0.01	3.31	15.58	99.91
ZK3402-8	300.0	0.03	1.41	69.01	5.53	0.08	0.03	0.01	3.01	0.01	6.40	14.40	99.92
ZK3402-9	300.3	0.02	1.38	69.35	5.87	0.09	0.03	0.01	2.91	0.01	5.73	14.51	99.91
ZK3402-10	300.6	0.03	4.17	51.55	14.74	0.11	0.03	0.01	2.42	0.04	14.51	12.28	99.89
ZK3402-11	302.6	0.07	4.77	35.75	31.09	0.06	0.29	0.05	1.93	0.03	13.81	12.06	99.91
ZK3402-12	303.5	0.11	3.80	35.99	35.35	0.07	0.66	0.08	1.90	0.02	9.49	12.46	99.93
ZK3402-13	303.9	0.20	3.58	34.92	36.40	0.08	1.71	0.10	1.65	0.02	9.90	11.38	99.94
ZK3402-14	305.0	0.28	3.34	34.29	36.64	0.09	2.57	0.10	1.68	0.02	10.72	10.19	99.92
ZK3402-15	305.5	0.35	2.74	32.97	37.88	0.10	4.13	0.13	1.36	0.02	11.5	8.77	99.95
ZK3402-16	307.3	0.63	1.48	33.97	43.01	0.09	6.08	0.17	1.60	0.01	4.56	8.33	99.93
ZK5604-2	521.3	0.10	0.79	50.80	29.15	0.05	0.17	0.01	1.88	0.01	2.52	14.48	99.96
ZK5604-3	523.5	0.11	0.30	37.58	43.87	0.06	0.11	0.04	2.17	0.01	1.25	14.40	99.90
ZK5604-5	525.3	0.09	0.25	35.33	42.21	0.06	0.12	0.07	1.40	0.01	4.75	15.70	99.99

Table 2. *Cont.*

Sample	Deep (m)	Na_2O	MgO	Al_2O_3	SiO_2	P_2O_5	K_2O	CaO	TiO_2	MnO	Fe_2O_3	LOI	Total
ZK5604-6	526.0	0.35	0.28	36.55	44.46	0.06	0.63	0.08	1.42	0.01	2.01	14.12	99.97
ZK5604-7	528.4	0.05	2.64	30.34	30.80	0.06	0.01	0.08	1.47	0.07	23.54	10.85	99.91
ZK5604-8	529.9	0.07	0.85	35.39	41.35	0.05	0.09	0.10	1.41	0.01	6.13	14.48	99.93
ZK5604-9	531.3	0.27	2.84	28.54	34.89	0.15	3.92	0.15	1.24	0.04	19.6	8.32	99.96

(LOI = loss on ignition at 1000 °C; Fe_2O_3 T = total iron expressed as Fe_2O_3).

Table 3. Trace element analysis results of bauxite, Huanglong Formation ash and Hanjiadian Formation shale.

Sample		Deep (m)	Li	V	Zr	Hf	Nb	Ta	Ni	Cr	Ga	Sr
ZK14904-4		386.7	524.1	328.2	526.5	13.6	51.6	3.4	3.2	335.4	55.7	230.0
ZK14904-5		387.0	731.2	325.7	467.1	13.3	39.5	2.8	4.8	351.5	64.9	256.4
ZK14904-6		387.1	232.0	502.5	741.4	25.4	114.6	7.3	16.1	383.9	111.6	90.6
ZK14904-7		387.9	265.5	516.9	714.5	22.8	89.8	6.5	23.8	465.5	112.3	81.2
ZK14904-8		388.1	194.5	456.9	471.4	13.1	60.9	4.0	16.2	289.9	86.7	100.5
ZK14904-9		388.6	185.8	546.5	525.2	16.1	64.4	4.7	14.6	620.5	96.0	130.4
ZK14904-10		389.0	231.7	494.9	467.3	14.1	57.5	4.0	21.8	407.1	81.6	102.4
ZK14904-12		390.3	87.8	263.2	458.1	14.4	67.9	4.5	5.4	241.7	78.6	117.2
ZK14904-13		390.5	84.7	270.0	468.9	14.9	69.0	5.0	5.4	239.1	80.8	109.5
ZK14904-14		390.9	167.7	303.9	456.5	13.3	58.1	4.3	8.0	200.8	74.4	57.9
ZK14904-15	Bauxite	391.6	172.8	329.0	1835.0	20.9	98.0	7.0	7.7	394.4	72.0	171.2
ZK14904-16		392.1	240.8	612.2	624.5	19.1	73.5	5.4	13.0	387.1	88.8	63.7
ZK14904-17		393.2	190.2	319.7	493.2	14.3	64.8	4.8	20.4	209.9	83.2	75.7
ZK14904-19		393.4	217.5	252.5	471.3	12.4	53.2	3.8	51.6	157.5	73.3	140.0
ZK14904-20		393.5	299.4	304.6	330.1	8.9	42.4	2.9	97.8	364.2	79.5	155.6
ZK14904-21		394.1	525.1	179.6	294.2	8.1	33.3	2.3	312.9	84.1	34.0	235.3
ZK14904-22		395.3	413.0	178.2	289.8	8.3	32.0	2.3	238.1	108.8	34.5	261.2
ZK14904-23		396.5	517.1	230.5	323.8	8.9	35.3	2.5	250.5	148.4	40.4	224.5
ZK14904-24		397.6	540.4	193.2	358.4	9.7	37.9	2.6	297.0	133.9	42.7	205.7
ZK14904-25		398.3	690.5	287.4	366.9	10.1	38.6	2.7	225.3	229.8	40.9	194.4
ZK14904-26		398.8	150.4	375.2	519.2	15.8	75.1	5.3	10.7	258.3	84.9	173.0
ZK14904-27		399.6	694.7	176.7	419.1	13.0	55.3	3.8	332.2	212.6	65.5	161.9
ZK14904-28	S_1h_j	401.9	70.7	221.7	173.1	5.0	21.0	1.5	90.2	155.1	40.3	226.9
ZK202-2		199.6	54.7	238.2	813.6	25.6	109.2	6.7	3.7	372.4	100.3	23.4
ZK202-3		201.7	550.9	431.3	462.2	9.7	44.1	2.6	75.7	171.5	43.5	80.9
ZK202-4	Bauxite	202.3	368.1	252.3	442.4	9.8	41.4	2.5	137.1	187.9	25.4	91.7
ZK202-5		203.5	461.2	118.4	375.6	8.8	38.1	2.7	202.7	148.0	43.5	54.1
ZK202-6		204.8	468.0	221.4	387.8	8.9	33.0	2.2	165.9	189.1	35.7	154.5
ZK202-7	C_2h	206.8	2.3	20.7	19.2	0.8	0.9	0.1	24.0	5.2	1.3	467.8
ZK3402-3		297.7	647.0	173.2	576.8	17.1	68.4	4.5	4.9	619.7	76.2	147.8
ZK3402-4		298.3	534.5	144.1	485.2	13.0	44.4	3.0	13.0	511.9	65.6	95.4
ZK3402-5		298.4	654.3	193.5	450.3	12.0	48.1	3.1	11.9	504.9	67.3	143.5
ZK3402-6		299.6	42.1	353.4	576.8	17.4	63.3	4.6	5.7	799.4	116.1	142.0
ZK3402-7		299.8	51.6	420.6	900.3	23.2	91.8	5.8	12.1	821.4	131.1	48.0
ZK3402-8		300.0	77.6	408.8	884.6	17.4	63.2	4.3	8.4	786.2	110.3	53.1
K3402-9	Bauxite	300.3	86.4	358.8	532.9	17.2	63.0	4.5	11.3	754.1	115.3	72.8
ZK3402-10		300.6	603.9	338.6	498.6	14.4	55.4	3.8	48.1	553.8	83.3	173.9
ZK3402-11		302.6	1239.9	309.9	412.5	12.2	45.6	2.9	114.0	489.2	54.1	113.0
ZK3402-12		303.5	1139.5	297.5	342.8	11.9	42.9	3.0	185.4	297.5	55.0	166.1
ZK3402-13		303.9	965.0	335.8	346.1	10.0	37.9	2.6	196.1	335.8	52.9	200.6
ZK3402-14		305.0	953.8	443.4	444.7	10.9	40.1	2.7	161.2	443.4	48.0	210.5
ZK3402-15		305.5	876.6	338.8	310.8	8.8	29.8	2.1	120.4	338.8	51.0	238.2
ZK3402-16		307.3	500.0	319.5	344.5	10.0	36.1	2.4	90.4	319.5	34.6	277.6

Table 3. *Cont.*

Sample		Deep (m)	Li	V	Zr	Hf	Nb	Ta	Ni	Cr	Ga	Sr
ZK3402-17	S_1h_j	307.8	134.2	311.1	344.8	9.0	34.2	2.2	104.8	311.1	41.2	314.4
ZK3402-18		308.6	53.2	150.7	178.9	4.9	23.4	1.6	74.3	150.7	37.9	179.4
ZK5604-2	Bauxite	521.3	5261.7	487.2	484.1	12.8	43.4	2.8	32.4	350.0	50.6	85.7
ZK5604-3		523.5	968.1	189.7	491.8	13.7	50.7	3.4	93.1	265.2	27.9	91.2
ZK5604-5		525.3	383.9	128.6	277.0	8.0	31.4	2.0	99.5	98.0	26.8	66.4
ZK5604-6		526.0	349.2	125.9	279.3	7.8	32.7	2.1	114.0	113.3	34.1	87.4
ZK5604-7		528.4	800.1	193.3	292.8	8.4	32.8	2.2	159.4	180.6	67.1	82.8
ZK5604-8		529.9	576.0	167.5	300.9	8.3	32.9	2.2	77.9	163.3	27.2	80.2
ZK5604-9		531.3	147.8	164.2	297.9	8.1	27.8	1.9	95.5	152.9	36.4	337.4
ZK5604-10	C_2h	532.8	41.0	28.7	47.5	1.2	4.9	0.3	60.1	28.8	7.5	282.3
ZK3228-3	Bauxite	621.2	1664.6	310.7	587.9	17.5	57.8	3.3	14.8	404.7	85.7	101.0
ZK3228-4		621.5	1318.7	334.8	653.6	22.2	84.6	4.9	11.6	777.2	140.4	103.2
ZK3228-5		621.6	6.7	303.9	876.4	30.8	116.8	6.8	6.1	667.4	135.7	55.2
ZK3228-6		622.6	4.8	297.3	866.8	32.0	114.9	7.0	6.1	648.5	135.1	53.8
ZK3228-7		623.4	97.5	325.3	558.4	21.7	82.8	5.3	38.4	369.3	98.3	79.4
ZK3228-9		624.5	488.9	170.0	391.1	9.8	36.1	2.5	102.6	193.0	40.1	320.6
ZK3228-12	C_2h	626.9	1.0	24.4	1.0	0.0	0.2	0.0	27.6	2.1	0.2	127.8
ZK3228-13		627.3	1.0	27.3	4.8	0.1	0.7	0.1	26.5	3.6	1.0	108.1
ZK3228-14		627.9	6.4	36.6	57.5	2.1	3.4	0.4	29.5	19.6	4.4	203.1
ZK3228-15	S_1hj	628.5	30.0	128.8	181.2	5.1	17.5	1.3	80.8	96.1	21.9	121.9

In addition, scandium, germanium, lithium, vanadium, tungsten, zirconium and other elements found in some bauxite deposits have also reached the industrial grade requirements. The average grade of Sc in bauxite in Guizhou is 45.4×10^{-6}, and the highest is 1539×10^{-6}. Its content is generally one to four times the average content of scandium in bauxite in the world (Sc_2O_3 is 38×10^{-6}) and it is, therefore, a potential scandium resource. The Linao, Xiaoshanba, Maige and Wuli bauxite deposits in central Guizhou have a higher scandium content, with Sc_2O_3 ranging from 28.7×10^{-6} to 75.2×10^{-6}, averaging 52.85×10^{-6}, while those in the Changchong and Shizishan bauxite deposits range from 21.0×10^{-6} to 48.2×10^{-6}, with an average of 31.53×10^{-6}. The Goujiang bauxite deposit in northern Guizhou ranges from 29.2×10^{-6} to 47.2×10^{-6}, with an average of 37.07×10^{-6}. However, these associated resources have not been investigated and studied in detail before. With the development of national technology in recent years, it is urgent to identify these important associated resources.

At present, among the associated elements of bauxite in Guizhou, lithium has the largest resource reserves, with the exception of gallium. Previous studies have shown that more than 100,000 tons of associated lithium resources have been found in the two bauxite deposits of Dazhuyuan and Wachangping in the Wuzhengdao area. In the Wachangping Bauxite Mine of Wuchuan County, the bauxite resources in the whole area are (332 + 333) 43.97 million tons, of which the controlled economic resources are (332) 5.57 million tons, and the associated Ga metal resources are (332 + 333) 7372 tons, of which (332) 1128 tons have an average grade of 0.01~0.03. The total amount of associated Li metal is 69,188 tons, including (332) 4362 tons with a grade of associated Li_2O_5 of 0.1~0.5. The bauxite in Dazhuyuan is associated with Ga, W, Li, Zr and other elements. The bauxite resource in the whole area is 63.3516 million tons, the associated rare metal Ga resource is 5448.25 tons, the Ga grade is 0.0050%~0.0135%, the average grade is 0.0086%, and the associated rare metal lithium (Li_2O) resource is 0.97 tons. The Li_2O grade is 0.020%~0.180%, with an average grade of 0.0984%, and the Zr grade is 0.0560%~0.1612%, with an average of 0.0818%. ∑RE2O3 is 0.0161%~0.0430%, with an average of 0.0318%. Wang Denghong et al. found, through the analysis and study of 81 drilling core engineering samples in the Dazhuyuan mining area, that the average W content in the whole area is 0.018%, the high content

of tungsten is distributed in the east wing of the Liyuan syncline, and the WO_3 content in some drilled bauxite reached 0.331%, which exceeds the boundary industrial grade of independent tungsten ore (scheelite deposit 0.15%, wolframite deposit (0.12%). The distribution of lithium in the whole Liyuan syncline is higher in the west wing than in the east wing, and higher in both wings than in the core, showing a trend opposite to the change in Al_2O_3 content, and the overall content exceeds the industrial grade requirements of lithium (560 ppm). However, the enrichment rules of tungsten and lithium in bauxite are still unclear, and WO_3 and Li_2O may have different enrichment mechanisms [21–24].

3.2. Mineral Characterization

The comprehensive analysis shows that the main minerals of Wuzhengdao bauxite are diaspore, kaolinite, chlorite and illite, with a small amount of heavy minerals such as anatase, zircon and rutile, a small amount of quartz and feldspar, and a certain amount of pyrite in some samples. The binary structure of bauxite is obvious. Generally, the diaspore content in the middle and upper part is 40–95%, and the rest is mainly kaolinite, chlorite, illite and other clay minerals. The bauxite reaching industrial grade is mostly concentrated in this section. The lower part is dominated by clay minerals, with a diaspore content of 5–40% and a clay mineral content up to 95%. The dense bauxite is light gray-black, and the semi-earthy bauxite is light gray-white. Both the dense bauxite and the semi-earthy bauxite are relatively pure in texture. The dense baxite is smooth and hard, while the semi-earthly baxite is rough and loose. Both the dense and semi-earthy structures are of muddy texture, and the grain size of both is of clay grade. The content of Al_2O_3 in dense bauxite is lower than that in semi-earthy bauxite, and the color of semi-earthy bauxite is mostly white, which reflects the strong iron removal in the later stage. The clastic bauxite particles are coarse, and the clastic components are mainly diaspore, kaolinite, chlorite, illite and other clay minerals, and the largest clastic particles can reach 2 cm. Clastic particles are poorly sorted, and particles of different size fractions are mixed and stacked together. Fragments include breccia and well-rounded gravel fragments. Oolitic structure (here refers to spheroid with concentric layers) is common in bauxite in the Wuzhengdao area, with obvious or indistinct concentric layers and no radial structure. Epidermal oolitis mostly has a coarse clastic core, which is rounded on one side and angular on the other. The oolite is mainly composed of diaspore and clay minerals (chlorite, kaolinite, illite, etc.), and some are pyrite, limonite, hematite, carbonaceous and siliceous. Oolitic grains are closely related to clastics, and many formed and incompletely formed oolitic grains are accumulated inside the clastics, which reflects the genetic relationship between oolitic grains and clastics. Diaspore is mostly cryptocrystalline, and the crystalline form of diaspore is often clustered. The formation of clastics is caused by the weathering and mud cracking of clay minerals. After the clay minerals such as kaolinite are broken, breccia is formed in situ or gravels are formed by short distance transportation. The heavy mineral assemblage of Wuzhengdao bauxite in northern Guizhou is dominated by weathering debris, zircon, limonite and rutile. The heavy mineral assemblage of bauxite in northern Guizhou is similar to that of the underlying strata, which indicates that the underlying strata provided ore-forming materials for the formation of bauxite. The bauxite in northern Guizhou contains some stable heavy minerals such as spinel and monazite, which are not found in the underlying strata, indicating that there are other rocks besides the underlying strata that provide ore-forming materials for the formation of bauxite. The stable heavy minerals from the parent rocks of magmatic rocks have undergone a certain degree of transportation and abrasion, and there is a certain degree of hydrodynamic action in the local bauxite mineralization process (Figures 2–4).

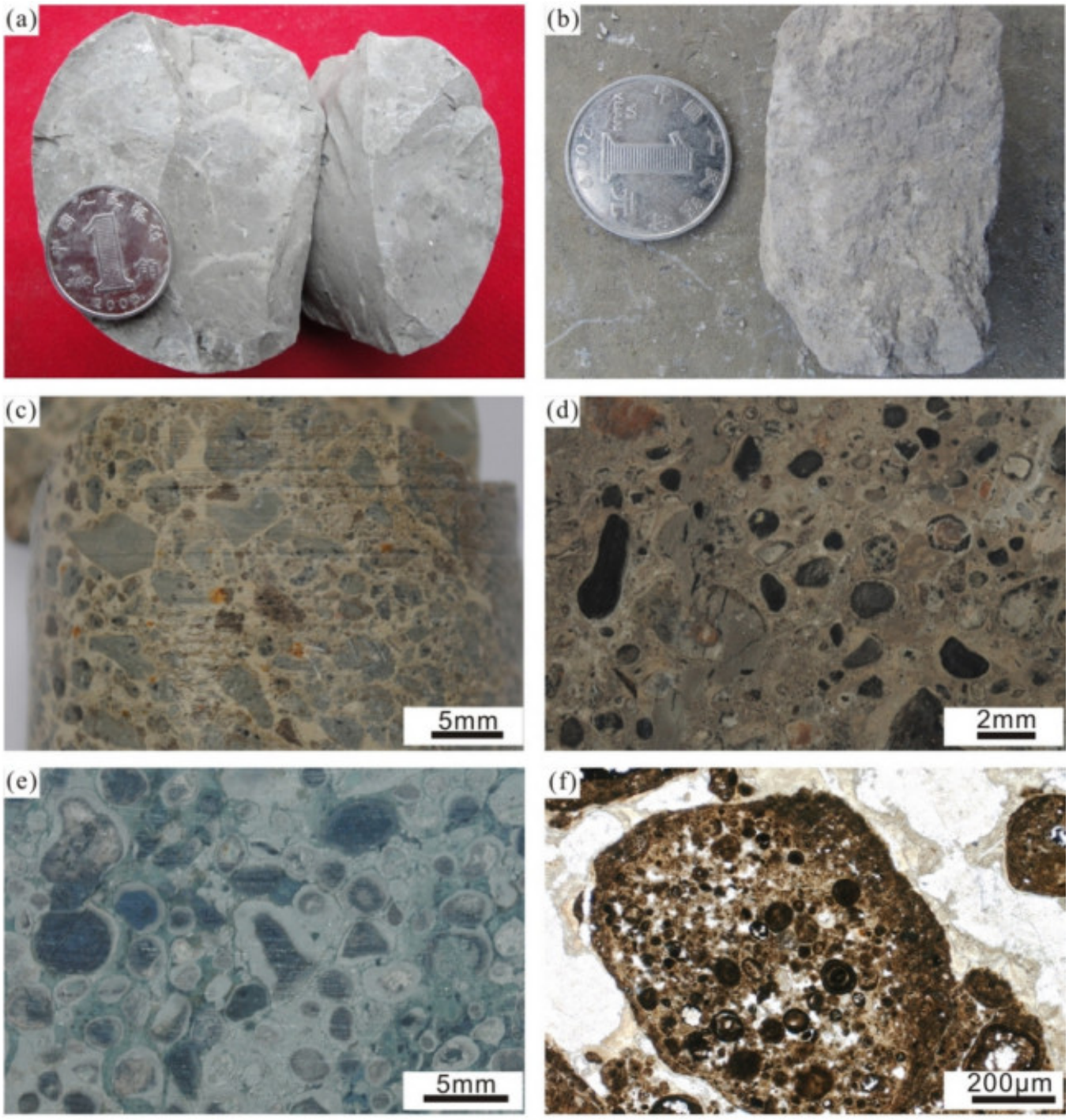


Figure 2. Field hand specimen and microscopic observation. (**a**)–(**c**) Bauxite ore; (**d**)–(**f**) from Photograph of bauxite mine identified under microscope.

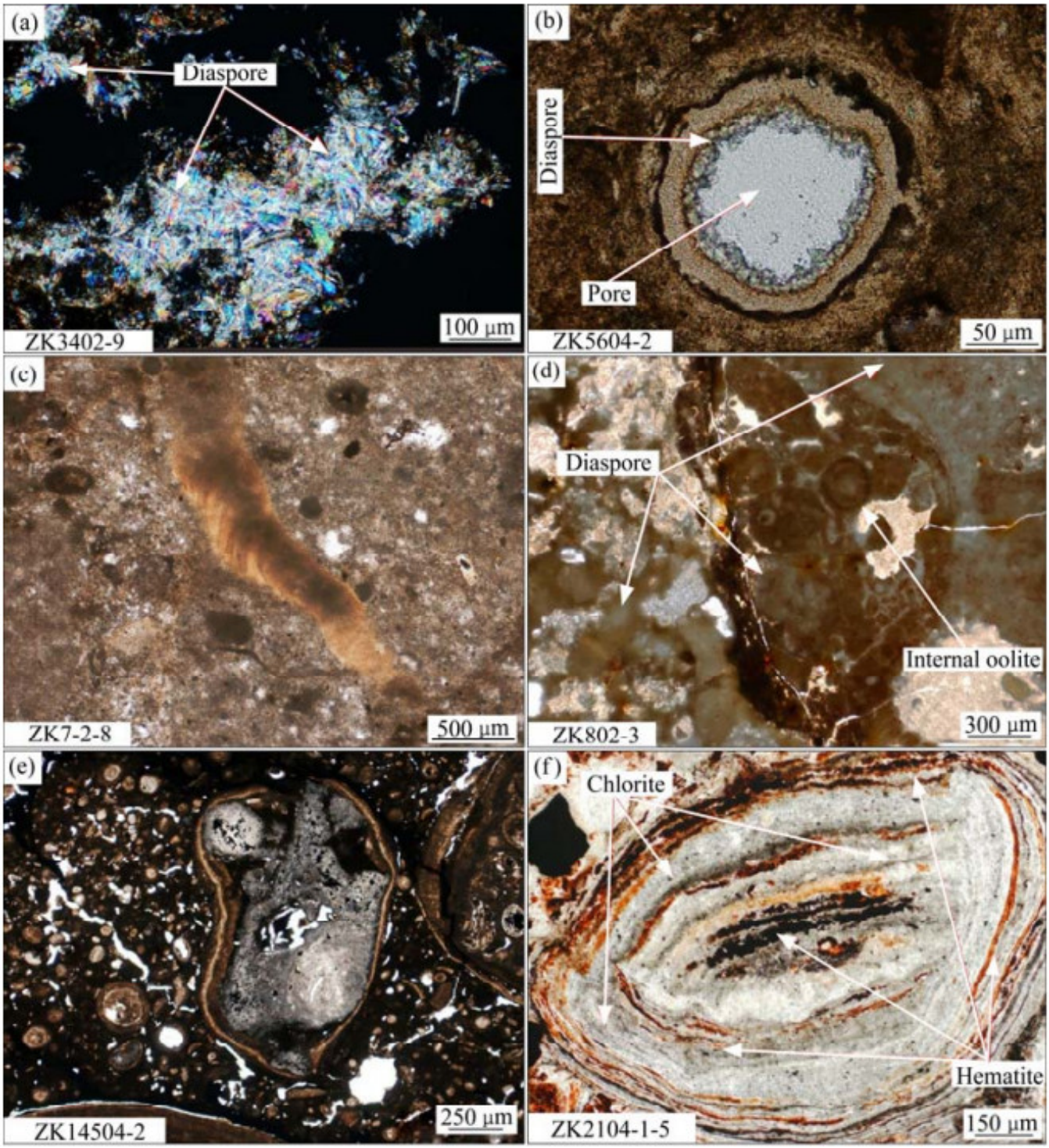


Figure 3. Features of bauxite (drilling samples) under optical microscope. (**a**)–(**f**) Single-polarized light of Oolitic and earthy ores.

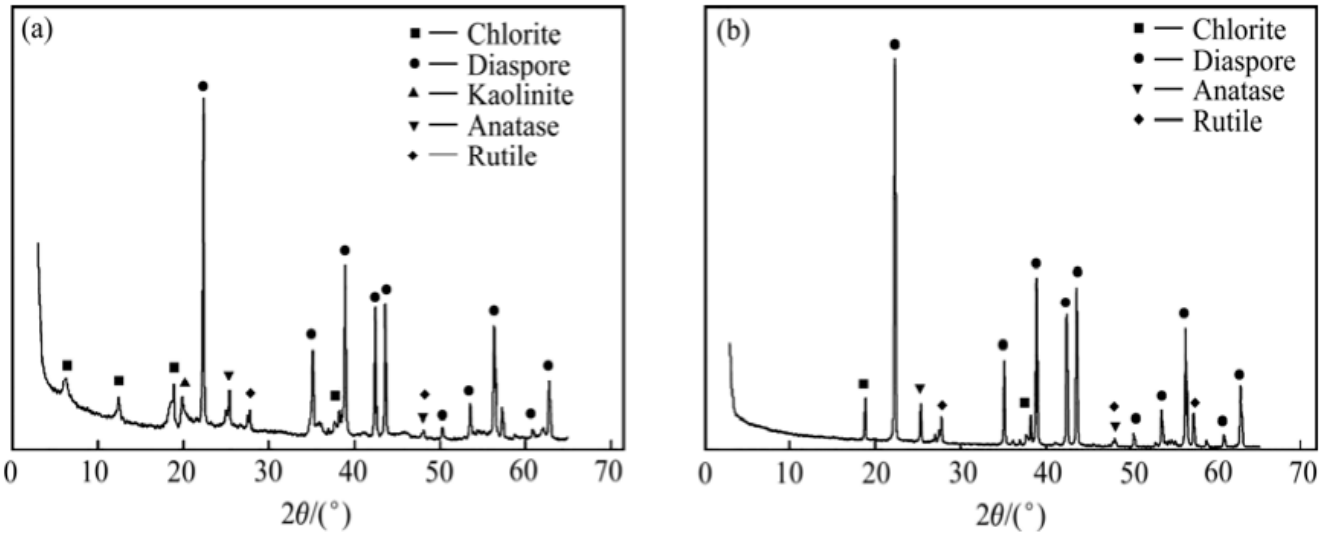


Figure 4. XRD patterns of bauxite: (**a**) ZK3228-6; (**b**) ZK3228-8.

3.3. Chemical Characterization

3.3.1. Major Element Characterization

The major elements of bauxite are Al_2O_3, SiO_2 and TFe_2O_3, followed by MgO and TiO_2. The content of Al_2O_3 and SiO_2 varies greatly, and there is a negative correlation between them, while there is a good positive correlation between TiO_2 and Al_2O_3. In the weathering process, Ti element remains stable, Si element migrates and is lost in large quantities, Al element has a certain loss but is relatively enriched, and alkali metal elements experience the most severe loss. After deposition, the bauxite was exposed to the earth surface and leached, large amounts of Si and Fe in the middle and upper bauxite were lost, and the alkali metal elements basically disappeared (Table 2).

3.3.2. Trace Element Characterization

Some trace elements are enriched in bauxite (Tables 3 and 4), with the highest Zr value of 1835 ppm, Cr, V and Li values almost all above 150 m; a few samples between 80–100 ppm; and most samples with Sr content above 70 ppm. The Zr content ranges from 277 to 1835 ppm, with an average of 510 ppm, showing an obvious positive anomaly with a large variation range, and the Zr content decreases gradually from the top to the bottom of the profile. The Hf value is relatively stable at 7.8–32 ppm, with an average of 14.3 ppm. Except for ZK14904, the Hf content in other boreholes is high in the middle and upper parts and low at the bottom, and the Hf content in ZK14904 shows multiple rising and falling cycles. The Hf content of ZK202 and ZK5604 in the north is less than 10 ppm, except for a few samples at the top, which is significantly less than the Hf content of other boreholes. The Hf content in ZK3228 in the middle of the study area is generally high, with an average of 22.3 ppm. The Nb content ranges from 27.8 to 116.8 ppm, with an average of 56.5 ppm; the whole is relatively stable; there is a decreasing trend from the top to the bottom of the borehole; and the law on the plane is not obvious. The content of Ta is between 1.9–7.3 ppm, which is relatively small and stable. The average value of ZK202 in the north is 3.3 ppm, and the average value of ZK5604 is 2.4, both of which are less than the average values of ZK3402 and ZK14904 in the south. The average content in ZK3228 in the middle is 5.0 ppm, which is the highest in all boreholes. The Cr content is relatively high at 84–821 ppm, with an average of 357 ppm. The Cr content is significantly reduced from the top of the borehole to the top in the vertical direction and from north to south in the plane. The Ni content ranges from 3.2 to 332.2 ppm, with an average value of 81 ppm. The range of variation is very large, and the profile shows an overall upward trend from the top to the bottom. The content of ZK3228 is generally low, with an average value of 29, which is the smallest of all boreholes. Except for ZK3228, the average value of other boreholes decreases gradually

from north to south. The contents of Zr, Hf, Nb, Ta and Cr increase gradually from north to south in the plane, and decrease gradually from the top to the bottom in the vertical profile. The contents of Zr, Cr and Nb are relatively high; Hf and Ta are relatively low; and Ni is relatively unique. The content variation in Ni in the horizontal and vertical directions is contrary to that of other elements, and the content of Ni in each sample is very different. Zr, Hf, Nb and Ta are positively correlated with TiO_2, and the correlation is better than that of Al_2O_3, indicating that Zr, Hf, Nb and Ta have been kept in a relatively stable state during the mineralization of bauxite [24–30].

Table 4. Analysis results of Ga, Li and rare earth elements.

Sample	Ba	Dy	Er	Eu	Ga	Sm	Sn	Sr	Ta	Tb	Th	Tm	U	V	W	Y	Li	Sc
	μg/g	μg/g	μg/g	μg/g	μg/g	μg/g	μg/g	μg/g	μg/g	μg/g	μg/g	μg/g	μg/g	μg/g	μg/g	μg/g	μg/g	μg/g
C2h-1	129.0	5.81	3.03	1.21	2.4	4.72	1	578	0.1	1.07	1.9	0.35	10.10	28	<1	48.3	6.0	3.1
S1hj-1	680.0	13.40	7.08	3.34	31.2	17.10	5	350	1.7	2.50	39.0	0.93	8.14	148	3	81.8	36.8	19.5
S1hj-2	512.0	4.81	2.79	1.16	25.0	6.39	4	209	1.1	0.83	19.6	0.44	4.22	135	2	27.9	26.6	14.8
Zky82909-1	11.0	0.17	0.15	0.04	0.6	0.24	<1	1770	0.1	0.03	0.7	0.03	5.12	27	<1	1.6	5.3	0.8
Zky82909-2	576.0	5.79	3.47	1.71	44.3	8.41	6	419	1.9	1.04	30.6	0.55	16.40	458	3	31.8	80.2	23.5
Zky82909-3	751.0	8.52	4.46	5.55	53.2	33.60	9	278	3.0	1.73	36.6	0.69	14.15	291	5	39.7	650.0	29.2
Zky82909-4	356.0	6.32	4.57	1.46	55.8	5.54	12	461	4.0	1.02	51.8	0.83	16.20	326	7	36.5	2160.0	33.8
Zky82909-5	226.0	11.05	7.27	3.75	159.5	19.90	17	643	4.8	1.90	93.7	1.26	18.60	691	22	61.7	281.0	39.7
Zky82909-6	22.2	12.90	8.87	1.74	120.5	7.79	22	246	6.4	1.91	92.8	1.47	21.90	641	9	77.1	8.5	38.9
Zky82909-7	21.1	8.96	5.61	3.19	106.5	17.30	16	373	4.0	1.64	59.2	0.94	16.15	397	7	50.4	39.8	32.4
Zky82909-8	89.8	6.44	3.61	3.24	55.2	14.70	10	381	2.8	1.19	39.7	0.61	9.09	195	5	31.5	660.0	32.6
Zky82909-9	306.0	5.27	2.96	1.77	28.5	4.86	7	165	1.9	0.86	26.2	0.48	7.28	219	3	28.6	690.0	37.7
Zky82909-10	242	6.27	4.08	2.62	67 6	12.40	12	226	3.3	1.12	48.1	0.65	11.60	299	6	35.0	2160.0	31.1
Zky82909-11	20.2	8.96	5.91	1.29	125.0	5.43	15	79	4.4	1.40	65.5	0.92	13.10	656	8	54.7	57.4	35.3
Zk15-2-1	200.0	211.00	98.40	46.50	44.8	241.00	3	388	1.4	36.90	19.2	12.50	59.60	218	2	1200.0	1210.0	90.6
Zk15-2-2	87.9	9.64	6.12	3.86	53.0	19.20	9	406	2.3	1.76	33.8	1.03	30.00	503	8	44.7	1120.0	40.7
Zk15-2-3	124.0	14.55	9.60	1.67	70.8	5.51	11	119	3.9	2.11	56.9	1.50	19.35	510	17	86.5	1370.0	42.8
Zk15-2-4	142.5	31.40	18.50	4.05	117.0	13.90	15	164	6.9	4.66	94.3	2.62	42.90	762	8	198.5	284.0	50.6
Zk15-2-5	16.2	23.70	13.75	3.51	168.5	12.95	13	135	5.0	3.82	70.0	1.95	45.20	723	6	135.0	5.3	42.5
Zk15-2-6	15.0	21.50	13.20	2.41	158.5	8.16	16	78	4.5	3.28	89.8	1.91	54.90	723	5	120.0	3.1	46.8
Zk15-2-7	806.0	5.69	4.39	1.44	27.9	8.14	9	355	2.8	0.81	37.3	0.78	9.47	336	4	36.0	1500.0	32.3
Zk15-2-8	540.0	13.00	5.38	7.44	28.5	51.70	7	447	2.0	3.33	30.9	0.82	10.50	429	3	60.8	910.0	27.1
Zk15-2-9	457.0	19.20	6.24	13.15	29.6	82.80	7	412	1.7	5.38	27.3	0.82	11.25	546	3	79.7	850.0	26.3
Zk15-2-10	35.1	21.30	10.55	3.45	2.9	11.35	1	274	0.1	3.64	1.1	1.22	3.03	37	<1	181.5	9.0	7.1
Zk15-2-11	39.3	1.12	0.63	0.30	2.1	1.25	1	318	0.1	0.19	1.5	0.09	7.09	24	<1	9.0	7.0	1.9
Zk403-1	29.6	7.20	4.48	0.67	48.3	1.98	16	65	4.4	0.98	43 2	0.72	10.85	137	9	43.9	690.0	19.0
Zk403-2	60.6	6.20	3.81	0.90	40.1	2.26	13	101	3.5	0.88	48.3	0.62	9.20	99	5	39.7	530.0	14.1
Zk403-3	11.2	9.77	6.54	0.86	76.4	3.33	17	63	5.3	1.34	54.4	1.02	13.45	216	8	58.8	101.0	26.1
Zk403-4	53.7	8.74	6.46	1.01	74.3	5.70	16	175	6.0	1.20	67.1	1.07	8.87	304	8	48.2	152.5	48.9
Zk403-5	8.9	8.28	6.34	0.97	75.2	5.88	17	224	5.1	1.23	63.5	1.08	7.88	313	7	45.2	198.0	45.7
Zk6A03-1	150.5	5.05	3.42	0.41	49.9	1.07	10	138	3.7	0.63	40.3	0.52	7.86	263	6	36.9	830.0	14.4
Zk6A03-2	14.6	9.97	7.42	0.44	104.5	1.42	14	42	5.1	1.13	92.6	1.12	11.35	270	29	71.1	130.5	23.6
Zk6A03-3	10.9	16.90	13.55	0.72	103.5	2.44	21	82	8.6	1.87	76.8	1.96	14.30	235	15	118.5	26.7	35.7
Zk6A03-4	10.1	11.20	9.47	0.51	96.8	2.01	17	61	5.8	1.17	64.7	1.36	11.10	205	9	77.5	16.7	32.0
Zk6A03-5	8.3	11.20	10.15	0.47	72.7	1.56	15	98	5.4	1.17	55.1	1.55	10.05	310	8	76.8	87.7	38.5
Zk6A03-6	7.9	12.50	11.90	1.31	72.1	5.55	14	62	4.8	1.61	57.8	1.97	7.84	243	7	80.0	116.5	34.4
Zk6A03-7	75.2	13.85	10.60	1.92	31.6	8.75	9	238	2.6	1.95	34.4	1.86	4.81	191	5	64.0	690.0	25.0
Zk1204-1	139.5	2.82	1.97	0.36	26.6	0.99	4	501	2.3	0.41	35.6	0.29	6.27	230	4	17.2	1290.0	21.5
Zk1204-5	84.3	6.44	5.02	0.50	23.7	2.01	9	103	3.1	0.78	35.9	0.76	8.07	93	3	31 3	420.0	33.6

4. Discussion

4.1. Data Analysis from the Literature

Through reading and secondary analysis of the documents related to the comprehensive utilization of gallium, lithium and scandium bauxite in northern Guizhou, it is known that, since the first discovery of bauxite in the Xiaoshanba area in 1941, after more than 70 years of prospecting and exploration work, 17 deposits have been explored, 25 deposits have been explored in detail, 36 deposits have been prospected, and 2 extra-large deposits and 12 large deposits have been proven. There are 40 medium-sized deposits and dozens of small deposits, and 21 integrated exploration blocks have been completed. The accumulative reserve of resources submitted by the whole province is approximately 12,900 million tons, accounting for about 25% of the national total, ranking second in the country. The bauxite deposits can be divided into three groups according to their genetic type: the lateritic type, the accumulative type and the sedimentary type, while the bauxite deposits found in Guizhou are all sedimentary-type bauxite formed by the original lateritic-type bauxites through surface-runoff transportation, migration and deposition in the nearby coastal, lagoon, swamp, peat swamp and other environments. It is a deposit dominated by mechanical clastic deposits, and the main aluminum mineral in the ore of the deposit is diaspore. The industrial types of ore include the low iron and low sulfur type, high sulfur type and high iron type.

By collecting and analyzing the correlation coefficient between lithium and other elements in bauxite deposits, no obvious correlation can be seen between the lithium content in bauxite deposits and Al_2O_3, SiO_2, Fe_2O_3, TiO_2, K_2O and other elements in ores. The Li content is not high in some deposits with high Al_2O_3 content. It shows that the content of Al_2O_3 is inversely correlated with the content of Li. In the study of Dazhuyuan bauxite, Wang Denghong also found that the content of lithium is inversely correlated with that of Al_2O_3 and found that the content of lithium in bauxite exceeds that in bauxite, which is also common in other lithium-bearing bauxite deposits. This may be determined by the nature of lithium itself, because bauxite is the product of a higher degree of weathering relative to bauxite; the higher degree of weathering makes the migration rate of lithium in bauxite too fast, and ultimately, leads to a lower content of lithium relative to bauxitic rock. However, it also provides conditions for the comprehensive development and utilization of the deposit. It can not only be used as an independent lithium resource, but also as a bauxite resource. The high lithium content can compensate for the low aluminum grade, which is very beneficial to the comprehensive evaluation and overall development of bauxite and lithium resources. A comparisons of the lithium content of different bauxite deposits is presented in Figure 4 The variation in lithium content in different bauxite deposits in northern Guizhou is obvious; the lithium content of most deposits can meet the requirements of the industrial grade, while the lithium grade of some deposits is too low. The Houcao and Xianrenyan bauxite deposits with low a lithium content are located in the Zunyi bauxite belt, and the deposits are formed in the carboniferous littoral swamp and peat swamp environments. The lithology of the basement is dolomite (with a small amount of shale) of the Lower Ordovician Tongzi Formation. It is mainly composed of upper Cambrian Loushanguan Group dolomite, and a small amount of Honghuayuan Formation limestone and Meitan Formation shale. Previous research data show that the ore-forming materials of bauxite in the Zunyi ore belt mainly come from the illite clay rock of the Ordovician Tongzi Formation and shale from the Meitan Formation, and it is speculated that the low lithium content may be related to its material source (Table 5).

Table 5. Lithium content of typical bauxite deposits in Guizhou.

Name of the Deposit	Lithology	Number of Samples (Piece)	Al_2O_3	SiO_2	Fe_2O_3	TiO_2	K_2O	Na_2O	Li (ppm)
Xinmin	Bauxite	11	67.10	10.69	3.04	2.79	0.20	0.53	360
	Bauxite	3	48.65	31.90	2.65	1.50	0.49	0.78	417
Yanping	Bauxite	4	54.40	20.28	8.32	2.21	1.05	0.63	1004
Peach Garden	Bauxite	3	52.71	20.62	6.73	1.25	0.34	0.72	539
Wachangping	Bauxite	8	46.72	27.51	5.53	1.31	0.49	0.71	656
	Bauxite	5	60.16	15.79	4.57	2.02	0.15	0.44	805
Rear Slot	Bauxite	30	65.63	11.26	3.88	2.91	2.08	0.03	73
Xianrenyan in Zunyi	Bauxite	30	63.83	7.02	11.91	2.80	0.48	0. 03	73
Correlation coefficient with Li			−0.240	0.227	0.001	0.261	0.093	0.441	1

At present, there are many studies on the enrichment mechanism of lithium in bauxite. The lithium content of bauxite ore is generally high, except for some samples with a large abnormal content, and the lithium content of other samples is high. The content of lithium in the low-quality coal seam and clay rock in the upper part of the bauxite layer decreased, while the lithium content in ferruginous clay rock increased significantly, and the lowest value appeared in quartz sandstone. Compared with mudstone and claystone in the area, it was found that the content of lithium in ferruginous mudstone or ferruginous weathering crust was relatively high, while the content of lithium in ferruginous mudstone was higher

than that in claystone, which indicates that the enrichment of lithium is related to rock properties, and the synchronous change in lithium content with iron content also indicates that there is a close relationship between lithium and iron. In the comparative study of lithium content in different types of rocks and ores in Dazhuyuan bauxite, it was found that the lithium content in oolitic bauxite decreased with the increase in aluminum content; there was no obvious correlation between lithium and aluminum in clastic, dense and semi-earthy bauxites; and lithium content did not enrich with the enrichment of aluminum. In Wachangping bauxite, Wuchuan, northern Guizhou, the lithium content in massive bauxite was higher than that in earthy bauxite, and the lithium content in bauxite was higher than that in bauxite–shale. Based on the distribution characteristics of lithium in various deposits, it can be seen that the lithium content in bauxite is basically inversely related to the aluminum content. As it may be affected by the source of metallogenic materials, the lithium content varies greatly in different ore belts and different deposits. In some deposits, it was found that it is not only bauxite that has a high lithium content, but lithium content was also high in lower grades of bauxite and claystone. In most bauxite deposits, the content of lithium was found to meet the requirements of the industrial grade, which indicates that in addition to the associated gallium element in bauxite in Guizhou Province having a high development and utilization value, the associated lithium element also has good comprehensive utilization prospects and is a potential lithium resource.

4.2. Enrichment and Migration of Associated Ga, Li and Rare Earth Elements

The REEs in the ore-bearing rock series show a certain variation in the vertical direction: from the top to the bottom, the contents of LREE, MREE, HREE and ∑REE show a gradual increasing trend. The chondrite-normalized REE patterns of the bauxite ore-bearing rock series show that LREE (La~Nd) is obviously enriched, MREE (Sm~Ho) is moderately to weakly enriched and HREE (Er~Lu) has a relatively flat feature with a distinct positive Ce anomaly. ZK5604 and ZK202 have higher δCe anomalies at the bottom of the profile. On the whole, the ore-bearing rock series shows a large LREE diversity and a small HREE diversity, and the LREE difference between the middle and upper parts of the section and the bottom is obvious, which may be the result of more REE loss in the middle and upper parts due to leaching transformation or downward migration and precipitation of REEs.

The bauxite and the Hanjiadian Formation shale not only have the characteristics of a Ce positive anomaly and LREE enrichment, but the trend in HREE change is also very consistent. Furthermore, the Huanglong Formation limestone shows an obvious Ce negative anomaly; HREE are far less than in the ore-bearing rock series, and the trend is inconsistent with bauxite. On the whole, the REE distribution pattern of bauxite is similar to that of Hanjiadian Formation shale, but obviously different from that of Huanglong limestone. The REE distribution pattern of the dense bauxite at the bottom of the ore series is very similar to that of Hanjiadian Formation shale, both of which have the characteristics of a Ce positive anomaly and LREE enrichment, and the HREE variation trend is basically the same; however, the overall trend is relatively flat. Although the REE distribution curve of the ore-bearing rock series of bauxite has changed to a certain extent after leaching, we cannot simply use the REE distribution curve to determine the provenance; however, it still shows that the ore-bearing rock series may be more closely related to the Hanjiadian Formation shale. REEs belong to the lanthanide series, and their chemical properties can be observed on the surface of minerals; therefore, LREE is more easily adsorbed on the surface of clay minerals, phosphate minerals, zircon, anatase, rutile and Fe, Mn oxides than HREE. Li is mainly adsorbed onto kaolinite, illite, montmorillonite, chlorite and other minerals in a dispersed state. Nb, Ta, Zr, Hf, V, Th and Ti, as inactive elements during bauxite mineralization, are easily adsorbed on the surface of clay minerals [31–35].

4.3. Metallogenic Process Analysis

Previous studies have shown that the laterization process is a necessary process for the formation of bauxite, and the ore-forming materials after the parent rock laterite are mainly kaolinite, hematite and other minerals, with some hard water stone. The mud shale of Hanjiadian Formation, limestone of Huanglong Formation and other rocks provided material sources for the formation of Wuzhengdao bauxite deposit in northern Guizhou, and these parent rocks provided original ore-forming materials for the formation of Wuzhengdao bauxite deposit after lateritization. The mineral-forming materials of Wuzhengdao bauxite deposit in northern Guizhou were deposited in a low-energy and reducing environment by means of colloidal transport or suspension transport. Fine-grained ore-forming materials are transported and deposited in the ore-forming basin, so the original sediments contain few clastic particles and are basically muddy materials that are mainly composed of clay minerals such as kaolinite and illite. During the transportation and deposition process, part of kaolinite may react with Mg^{2+} in the sea water and transform into chlorite. According to this, it is inferred that if the ore-forming parent material is directly consolidated into rock without other transformation after deposition, it should be clay rock. If the mass fraction of Al_2O_3 in the claystone is more than 40%, it will become dense bauxite. Therefore, the initial state of most ores of Wuzhengdao bauxite should be claystone, or claystone with a color, structure and composition similar to dense bauxite. The initial state of the ore is a muddy structure, the content of clastic particles is small, the color is light gray-grayish green, and the content of Al_2O_3 is low.

4.3.1. Mineralization

This work found that the oolitic minerals are mainly chlorite and diaspore, chlorite can be transformed from laterization products such as kaolinite and feldspar in a reducing environment, the sedimentary environment of bauxite is reducing, and the oxygen content decreases gradually from the top to the bottom of the profile in the leaching process, all of which can form chlorite. The formation of diaspore has always been controversial; usually, there are two views: the formation of high temperature and high pressure and the formation of normal temperature and normal pressure, but diaspore is not the main product of laterization. Wuzhengdao bauxite is formed under the transformation of transportation, deposition and leaching in the surface environment, that is, there is no high temperature and high pressure environment in the deposition and mineralization process of bauxite formation, so diaspore can only be formed under normal temperature and normal pressure. In addition, diaspore can be seen in Wuzhengdao bauxite, which is crystallized around the later dissolution pores. This is obviously the product at normal temperature and pressure after deposition, so the formation of diaspore at normal temperature and pressure is beyond doubt. The XRD analysis of the ore and the SEM image of the oolite show that diaspore is mostly associated with chlorite, and less with other minerals; in particular, high-grade bauxite is mostly associated with chlorite, which implies that the formation of diaspore is closely related to chlorite. In the acidic environment formed by leaching, kaolinite, feldspar and other minerals are transformed into diaspore and chlorite. Chlorite can be further transformed into diaspore by continuous leaching, thus, improving the ore quality.

Aluminum compounds are mainly diaspore and boehmite: diaspore is dominant and boehmite is only a small amount. There are many explanations as to the origin of diaspore: (1) Metamorphic origin: gibbsite becomes boehmite by dehydration, and boehmite becomes diaspore under shallow metamorphism. (2) Weathering genesis: gibbsite or kaolinite is directly transformed into diaspore at low temperature. (3) Diagenetic crystallization. There is no obvious metamorphism in Wuzhengdao bauxite, diaspore is in a transitional state with clay minerals such as chlorite and illite, and dissolution is often seen in the boundary and interior. At the same time, diaspore can be associated with hematite, limonite, pyrite and ilmenite. All these indicate that diaspore in the Wuzhengdao area is mainly transformed from other clay minerals under surface conditions. Diaspore is formed by desilication and iron removal from kaolinite and chlorite by leaching in the surface environment. In

the pores of bauxite, there are diaspore crystals with huge grains and complete crystal forms, which are formed by direct crystallization and may be formed during diagenesis. The quantity of boehmite in Wuzhengdao bauxite is small, which may be produced in the process of laterization and accumulated in the ore-bearing rock series of bauxite after transportation and deposition. There is a large amount of colloidal diaspore in Wuzhengdao bauxite. This part of diaspore is formed by the coagulation of aluminous colloid. It is obvious that these diaspores are the products of sedimentary period.

4.3.2. The Ore-Forming Process

On the basis of previous work, according to the ore-forming process of Wuzhengdao bauxite deposit in northern Guizhou, this paper systematically analyzes the formation process and sequence of main minerals, and the formation of minerals can be divided into the following stages: weathering period, syngenetic period (transportation and deposition period), penecontemporaneous period (intermittent exposure to the surface period), diagenetic period and supergene period. According to the analysis of hand specimens and scanning electron microscope, each mineral has a variety of forms, the boundaries between minerals are not clear, and there is a transitional evolution relationship between minerals, which proves that minerals are formed in different stages.

The weathering period mainly refers to the laterization of parent rock, which provides the most basic ore-forming materials for bauxite. The minerals formed in this period mainly include kaolinite, diaspore and anti-weathering heavy minerals such as ilmenite and zircon. Zircon and ilmenite in Wuzhengdao bauxite are rounded to a certain extent, indicating that they have undergone certain transportation, which suggests that zircon and ilmenite are products of the weathering period.

The contemporaneous stage refers to the stage from the transportation and deposition of bauxite into the basin to the compaction and diagenesis. At this stage, diaspore is transported to the sedimentary basin in the form of colloid, kaolinite is mainly transported in the form of suspension, part of kaolinite is transformed into chlorite in the process of transportation and deposition, and both kaolinite and chlorite can be transformed into diaspore. In the sedimentary basin, the residual hematite in situ is transformed into pyrite (locally, it is still hematite under relatively high energy and oxidation conditions, and the newly deposited pyrite is transformed into hematite). At this stage, the content of Al in the unconsolidated sediments has been greatly increased.

4.4. Comprehensive Utilization Analysis of Associated Ga, Li and Rare Earth Elements

4.4.1. Analysis of the Comprehensive Utilization of Ga and Li

Approximately 70% of Ga is dissolved and enriched in the mother liquor in the process of bauxite electrolysis. A total of 90% of Ga in the world comes from recovery from the electrolytic aluminum process, and the remaining 30% of undissolved Ga in bauxite remains in red mud. The recovery process of Ga includes fractional precipitation, electrochemical deposition, solvent extraction and ion exchange. Recent studies have shown that solvent extraction and ion exchange have a better extraction performance than other methods because of their simple process and lack of environmental pollution. There are few reports on the process of extracting Ga from red mud. Some scholars try to extract Ga from red mud via the acid-leaching ion exchange method. The leaching efficiency of Ga by hydrochloric acid, sulfuric acid and nitric acid is compared. The results show that the leaching efficiency of Ga by hydrochloric acid is the highest, which can reach 97. The optimum leaching conditions are as follows: the concentration of hydrochloric acid is 159 G/L, the leaching temperature is 55 °C, the leaching time is 4 H, and the ratio of liquid to solid is 8 mL/G, under which the leaching efficiency of Ga is 94.77%. Ga is then concentrated by iron removal and a recycling process, and the concentrated solution with a Ga content of 97.54% can be obtained by ion exchange treatment of the sixth circulating solution (Ga concentration of 20.52 mg/L).

The content of Li in the aluminum-bearing rock series in Guizhou is high and varies widely. In terms of the plane, the content of Li is generally high in the northeast and southwest metallogenic provinces and low in the middle metallogenic province. In terms of the profile, Li is mainly enriched in the dense bauxite (ore) in the upper part of the ore series. The continental lacustrine sedimentary environment with a warm and humid climate and strong weathering and leaching is favorable for the formation of clay minerals dominated by kaolinite, which promotes the isomorphism of Li^+ with Al^{3+}, Mg^{2+}, Fe^{3+} and Fe^{2+} to the greatest extent, or the adsorption and enrichment of Li^+ by clay minerals. With the increase in desilication and aluminum enrichment, a large amount of Li^+ is lost, resulting in the depletion of high-grade bauxite. Li^+ mainly comes from the underlying strata with a high background, which is consistent with the parent rock of bauxite mineralization, and part of it may also come from the overlying Li-rich strata. The enrichment degree of Li^+ is closely related to the background of the ore-forming parent rock. The enrichment characteristics of Li^+ in aluminum-bearing rock series show that lithium resources have good prospecting potential. Strengthening the process of mineralogy research and expanding laboratory research and industrial index demonstration are expected to transform lithium resources in aluminum-bearing rock series into available minerals.

4.4.2. Analysis of the Comprehensive Utilization of Rare Earth Elements

Bauxite is often associated with rare earth and other important strategic mineral resources, which has great potential economic value. Predecessors have studied the occurrence of rare earth elements in Wuzhengdao bauxite in northern Guizhou through chemical phase analysis, including the gradual separation of four phases, namely, the water-soluble phase, ionic phase, colloidal sedimentary phase and mineral phase, and the gradual separation of carbonates, organic matter, iron minerals, quartz and silicates. Rare earth elements in bauxite in northern Guizhou are mainly in the mineral phase and ionic phase; rare earth elements in the water-soluble phase and colloidal sedimentary phase are very few, and rare earth elements in the mineral phase mainly occur in silicate minerals. According to the mineral composition characteristics of bauxite in this area, clay minerals are considered to be the main carrier minerals of rare earth elements, which mainly occur in clay minerals (such as kaolinite and chlorite) in the form of isomorphism. Some rare earth elements are adsorbed by aluminum minerals (such as diaspore, boehmite, gibbsite, etc.) and clay minerals in a dispersed state.

REE-fluorocarbon is the most common REE mineral in karst bauxite. In these minerals, Ce plays a dominant role in rare earth elements. The existence of this mineral will significantly affect the shape of REE patterns and cause obvious Ce anomalies in ores. The mineral control of monazite can lead to the fractionation and enrichment of LREE relative to HREE. For example, four kinds of REE phosphate minerals are distinguished in Heishan bauxite: authigenic monazite, residual monazite, authigenic xenotime and residual xenotime, and these four kinds of phosphate minerals have different controls on different REEs. The LREEs of La, Pr, Sm, Gd and Dy are abundant in both monazites, and are more abundant in authigenic monazite. In addition, authigenic monazite has an obvious control effect on Nd, while residual monazite has an obvious control effect on Ce. Different from monazite, both xenotime and xenotime are rich in HREE (Gd, Dy, Er, Yb) and poor in LREE (La, Ce, Pr, Eu, Nd, Sm). The authigenic xenotime contains a small amount of V and Sc, while the residual xenotime does not. In addition, some low-solubility elements (e.g., Zr, Th, Ti, V, Ga) are concentrated in detrital zircon and monazite (Zr, Th), as well as in anatase (Ti, V) and hematite (Ga). Compared with bauxite, the enrichment factor of REEs in red mud is approximately 2, and the concentration of REEs in red mud may be between 500 and 1700 mg/kg. The extraction of REEs from red mud usually uses a hydrometallurgical or pyrolytic hydrometallurgical process with extensive use of solutions (mineral acids, CO_2, bioleaching, highly acidic ionic liquids), leaching, selectively dissolving REEs, and further enriching the mother liquor by ion exchange or solvent extraction [36–40].

In the red mud leaching solution, polyethyleneimine (PEI)-modified chitosan material (PEI–chitosan material) can be used as an effective adsorbent for La ions, and La ions can be easily separated from Al ions with a separation factor of 3.1. The adsorption behavior of a single metal showed that it had a rapid and effective adsorption capacity of 2.015 mmol/G for the La ion. The N atom forms a coordination bond with La by sharing an electron pair, thereby forming an eight-membered chelate ring. The PEI–chitosan material also showed excellent reusability with a regeneration efficiency of 90% after four cycles.

Sc is a typical rare and scattered lithophile element. The content of Sc_2O_3 in bauxite is generally between 40 and 150 μg/G. After the production of alumina, it can be enriched by more than 98% in red mud, and the highest content can reach 0. Therefore, red mud is usually used to extract Sc in the industrial production process. At present, the recovery process of extracting Sc from red mud is mainly divided into hydrometallurgy and pyro-hydrometallurgy. In hydrometallurgy, red mud is directly leached with high-concentration acid to cause Sc and impurity ions to enter the solution from the red mud. Then, Sc_2O_3 is obtained by ion exchange after extraction with an extractant and alkali back extraction, and finally, Sc is obtained by roasting. Pyro-hydrometallurgy is mainly to separate Fe, Al and Sc in red mud by repeated sintering, so that Sc can be enriched in white mud (the content of Sc in white mud is 2.65 times that in red mud). Sc is obtained by acid-leaching extraction (or ion exchange). Although the industrial processes of hydrometallurgy and pyro-hydrometallurgy are different, both gradually separate Sc from other metal ions, enrich Sc in solution by acid leaching, and then recover Sc by solvent extraction (ion exchange). In addition, approximately 98% of Sc can be extracted from P204 and P507 by acid leaching with phosphoric acid, hydrochloric acid, sulfuric acid and calcium fluoride under suitable conditions. In addition, special selective adsorbents such as the hydrophobic ionic liquid beryllium bis (trifluoromethylsulfonyl) imide (HbetTf2N), resin D201, and the organic system composed of D2EHPA and TBP play an important role in the extraction of Sc [41–44].

5. Conclusions

5.1. Urgent Demand for Science and Technology

Different from the shortage of bulk mineral resources (Fe, Al, Cu, etc.), China's strategic mineral resources have great potential, and their distribution is very distinctive in the global context. A thorough understanding of the metallogenic regularity of these minerals is of great significance to enrich the metallogenic theory, determine the resources available, meet the national demand for strategic mineral resources, and control the international supply and demand of these minerals. However, compared with other deposits, the research and development of these deposits in China generally started late, the metallogenic regularity has not been well grasped, the exploration depth of the existing deposits is shallow, and there are many virgin lands with mineralization but no exploration. For example, although rare/scattered elements are of great value in the national economy, in China, whether they are independent deposits of rare/scattered elements or rare/scattered metals as associated components of other minerals, their recognition, attention and development and utilization are far lower than for other mineral resources. On the one hand, people are bound by the traditional way of thinking that their highly dispersed geochemical properties determine that they are impossible to form deposits; on the other hand, due to technical, economic and other reasons, the rare/dispersed metals, which usually appear as associated components, are not fully utilized as a resource but are discarded as "waste rock" or "tailings", resulting in a great waste of resources. It is undoubtedly one of the important and effective ways of prolonging the life of a mine, reducing the production cost and increasing the benefit by researching and developing the independent or associated rare/dispersed metals [41–43].

More importantly, the formation of strategic mineral resources often has a special geological background and metallogenic process, which determines that strategic mineral resources have special metallogenic conditions and controlling factors. At the same time, the metallogenic theory, prospecting model and exploration technology needed for

its exploration are not identical to those of other types of deposits, which need to be studied by special metallogenic theory, establishing a targeted prospecting model and exploration techniques.

5.2. Accelerating Breakthrough Strategic Actions

Rare earth, scattered and rare metals found in Guizhou are often associated with phosphate ore, coal, lead–zinc ore, bauxite, basalt weathering zone, nickel–molybdenum polymetallic deposits or geological bodies. In recent years, with the steady progress of integrated exploration work, a series of prospecting achievements have been made in the comprehensive evaluation of mineral resources, especially for the associated minerals. Comprehensive evaluation has shown that associated gallium resources have equaled 52,162 tons, lithium resources 432,146 tons, cadmium resources 4714 tons and germanium resources 17,139 tons.

At present, due to the continuous downturn of the mining economy, the economic value of traditional minerals is declining year by year, and the investment in and development of the mining industry is almost stagnant. Improving the added value of minerals is the most important issue in the development of the mining economy. With the rapid development of emerging industries, the strategic value and status of "associated" minerals have been highlighted. To carry out the investigation and evaluation of associated mineral resources in the whole province can not only fully assess the distribution law of associated resources and determine the resource background, but also contribute to future mining development, especially the comprehensive utilization of associated resources. It is conducive to the transformation and upgrading of the mining economy and to achieving a major breakthrough in prospecting. This is not only in line with the national strategy, but will also help to ensure the rapid and stable development of the province's mining economy.

Author Contributions: Conceptualization, M.Z.; methodology, W.Y.; software, M.Z.; formal analysis, W.Y.; investigation, C.T. and W.Y.; writing—original draft preparation, C.T.; writing—review and editing, W.Y. and J.Y. All authors have read and agreed to the published version of the manuscript.

Funding: This research was supported by Guizhou Provincial Science and Technology Projects (Qian(2017)1410), the high-level talent introduction program for the Guizhou Institute of Technology (0203001018040).

Institutional Review Board Statement: Not applicable.

Informed Consent Statement: Not applicable.

Data Availability Statement: Not applicable.

Conflicts of Interest: The authors declare no conflict of interest.

References

1. Tao, C.; Min, Z. Characteristics of Heavy Mineral Assemblages in Bauxite Deposits in Northern Guizhou and Their Geological Significance. *Chin. J. Nonferrous Met.* **2021**, *31*, 1106–1119.
2. Lapparent, J.D.E. *Les Bauxites de la France Méridionale*; Imprimerie Nationale: Paris, France, 1930; pp. 1–187.
3. Du, Y.; Zhou, Q.; Jin, Z.; Ling, W.; Zhang, X.; Yu, J.; Wang, X.; Yu, W.; Huang, X. Research progress on basic geology and mineralization of bauxite in Wuzhengdao area, northern Guizhou. *Geol. Sci. Technol. Inf.* **2013**, *32*, 1–6.
4. Liu, Y.; Zhou, W.; Cheng, G.; Cui, T.; Long, H. Study on characteristics of ore-bearing rock series and metallogenic regularity of bauxite in Guizhou. *Acta Mineral. Sinica* **2016**, *36*, 289–294.
5. Lei, Z.; Weng, S.; Chen, Q.; Xiong, X.; Pan, Z.; He, X.; Chen, H. Lithofacies palaeogeography of the Dazhuyuan Age of the Early Permian in the Wuzhengdao area, northern Guizhou, and its ore-controlling significance for bauxite. *Geol. Sci. Technol. Inf.* **2013**, *32*, 8–12.
6. Cui, T.; Jiao, Y.; Du, Y.; Yu, W.; Ji, B.; Lei, Z.; Weng, S.; Jin, Z.; He, X. Palaeosalinity identification of bauxite formation environment in Wuzhengdao area, northern Guizhou. *Geol. Sci. Technol. Inf.* **2013**, *32*, 46–51.
7. Liu, C.; Jin, Z.; Guo, J. Sedimentary facies of freshwater sedimentary bauxite deposit in Wuzhengdao area, northern Guizhou. *J. Cent. South Univ.* **2015**, *46*, 962–969.
8. Wang, X.; Jiao, Y.; Du, Y.; Ling, W.; Wu, L. Rare earth element geochemical characteristics of bauxite in Wuzhengdao area, northern Guizhou. *Geol. Sci. Technol. Inf.* **2013**, *32*, 27–33.

9. Emmalou Van Tilburg, N. Why adults participate? *J. Ext.* **1992**, *30*, 12–13.
10. Thongmak, M. Inquiring into lifelong learning intention: Comparisons of gender, employment status, and media exposure. *Int. J. Lifelong Educ.* **2021**, *40*, 72–90. [CrossRef]
11. Zhang, Y.; Zhang, Y.; Wu, H.; Ding, X.; Ling, W.; Lei, Z.; Weng, S.; Ma, Q.; Du, Y. Micro-area element geochemical characteristics and metallogenic significance of oolitic bauxite in Wuzhengdao area, northern Guizhou. *Geol. Sci. Technol. Inf.* **2013**, *32*, 62–70.
12. Zhang, Y.; Ling, W.; Wu, H. Geochemical characteristics of different types of bauxite ores in northern Guizhou and their implications for mineralization. *Geol. Sci. Technol. Inf.* **2013**, *32*, 71–79.
13. Yin, K. Mineralization and metallogenic model of Wuzhengdao bauxite deposit in northern Guizhou. *Acta Sedimentol. Sin.* **2009**, *27*, 452–457.
14. Zarasvandi, A.; Carranza, E.J.M.; Ellahi, S.S. Geological, geochemical, and mineralogical characteristics of the Mandan and Deh-now bauxite deposits, Zagros Fold Belt, Iran. *Ore Geol. Rev.* **2012**, *48*, 125–138. [CrossRef]
15. Liu, X.; Wang, Q.; Deng, J.; Zhang, Q.; Sun, S.; Meng, J. Mineralogical and geochemical investigations of the Dajia Salento-type bauxite deposits, western Guangxi, China. *J. Geochem. Explor.* **2010**, *105*, 137–152. [CrossRef]
16. Wang, D.; Li, P.; Qu, W.; Yin, L.; Zhao, Z.; Lei, Z.; Wen, S. Discovery and comprehensive evaluation of tungsten and lithium in Dazhuyuan bauxite deposit, Guizhou Province. *Sci. China Earth Sci.* **2013**, *43*, 44–51.
17. Yu, W.; Du, Y.; Gu, S. Multi-stage leaching of Early Permian bauxite in Wuzhengdao area, northern Guizhou, and its ore-controlling significance. *Geol. Sci. Technol. Inf.* **2013**, *32*, 34–39.
18. Jin, Z.; Zou, L.; Zhang, L.; Zheng, M.; Han, Y. Metallogenic model and prospecting model of bauxite in Wu-Zheng-Dao area, Guizhou. *Acta Sedimentol. Sin.* **2018**, *36*, 914–926.
19. Calagari, A.A.; Abedini, A. Geochemical investigations on Permo-Triassic bauxite horizon at Kanisheeteh, east of Bukan, West-Azarbaidjan, Iran. *J. Geochem. Explor.* **2007**, *94*, 1–18. [CrossRef]
20. Liu, C.; Jin, Z.; Guo, J. Effect of sea level change on the enrichment and mineralization of sedimentary bauxite: A case study of bauxite in northern Guizhou. *Chin. J. Nonferrous Met.* **2018**, *28*, 985–993.
21. Anawati, J.; Azimi, G. Recovery of scandium from Canadian bauxite residue utilizing acid baking followed by water leaching. *Waste Manag.* **2019**, *95*, 549–559. [CrossRef]
22. Gu, J.; Huang, Z.; Fan, H.; Jin, Z.; Yan, Z.; Zhang, J. Mineralogy, geochemistry, and genesis of lateritic bauxite deposits in the Wuchuan–Zheng'an–Daozhen area, Northern Guizhou Province, China. *J. Geochem. Explor.* **2013**, *130*, 44–59. [CrossRef]
23. Narayanan, R.P.; Kazantzis, N.K.; Emmert, M.H. Process for Scandium Recovery from Jamaican Bauxite Residue: A Probabilistic Economic Assessment. *Mater. Today Proc.* **2019**, *9*, 578–586. [CrossRef]
24. Zhou, K.; Teng, C.; Zhang, X.; Peng, C.; Chen, W. Enhanced selective leaching of scandium from red mud. *Hydrometallurgy* **2018**, *182*, 57–63. [CrossRef]
25. Li, G.; Ye, Q.; Deng, B.; Luo, J.; Rao, M.; Peng, Z.; Jiang, T. Extraction of scandium from scandium-rich material derived from bauxite ore residues. *Hydrometallurgy* **2018**, *176*, 62–68. [CrossRef]
26. Zhu, X.; Niu, Z.; Li, W.; Zhao, H.; Tang, Q. A novel process for recovery of aluminum, iron, vanadium, scandium, titanium and silicon from red mud. *J. Environ. Chem. Eng.* **2020**, *8*, 103528. [CrossRef]
27. Mameli, P.; Mongelli, G.; Oggiano, G.; Dinelli, E. Geological, geochemical and mineralogical features of some bauxite deposits from Nurra (Western Sardinia, Italy): Insights on conditions of formation and parental affinity. *Int. J. Earth Sci.* **2007**, *96*, 887–902. [CrossRef]
28. Zhao, L.; Liu, X.; Yang, S.; Ma, X.; Liu, L.; Sun, X. Regional multi-sources of Carboniferous karstic bauxite deposits in North China Craton: Insights from multi-proxy provenance systems. *Sediment. Geol.* **2021**, *421*, 105958. [CrossRef]
29. Zhang, S.; Liu, X.; Zhao, F.; Liu, D.; Zou, Y.; Zhang, W.; Liu, X.; Li, L.; Zhao, L. Geological and geochemical characteristics of karst bauxite-bearing sequences in Xiabu area, Central Shanxi Province, North China. *J. Geochem. Explor.* **2021**, *230*, 106849. [CrossRef]
30. Yang, W.; Zhang, M.; Yan, J.; Chen, X. Zircon U-Pb Ages and Geochemistry of the Granite in the Xintianling Tungsten Deposit, SE China: Implications for Geodynamic Settings of the Regional Tungsten Mineralization. *Minerals* **2022**, *12*, 952. [CrossRef]
31. Onghena, B.; Borra, C.R.; Van Gerven, T.; Binnemans, K. Recovery of scandium from sulfation-roasted leachates of bauxite residue by solvent extraction with the ionic liquid betainium bis(trifluoromethylsulfonyl)imide. *Sep. Purif. Technol.* **2017**, *176*, 208–219. [CrossRef]
32. Zhang, X.; Zhou, K.; Wu, Y.; Lei, Q.; Peng, C.; Chen, W. Separation and recovery of iron and scandium from acid leaching solution of red mud using D201 resin. *J. Rare Earths* **2019**, *38*, 1322–1329. [CrossRef]
33. Zhang, M.; Yang, W.; Yang, M.; Yan, J. Guizhou Karst Carbon Sink and Sustainability—An Overview. *Sustainability* **2022**, *14*, 11518. [CrossRef]
34. Wang, W.W.; Pranolo, Y.; Cheng, C.Y. Recovery of scandium from synthetic red mud leach solutions by solvent extraction with D2EHPA. *Sep. Purif. Technol.* **2013**, *108*, 96–102. [CrossRef]
35. Lu, F.; Xiao, T.; Lin, J.; Li, A.; Long, Q.; Huang, F.; Xiao, L.; Li, X.; Wang, J.; Xiao, Q.; et al. Recovery of gallium from Bayer red mud through acidic-leaching-ionexchange process under normal atmospheric pressure. *Hydrometallurgy* **2018**, *175*, 124–132. [CrossRef]
36. Nayak, S.; Devi, N. Studies on extraction of gallium (III) from chloride solution using Cyphos IL 104 and its removal from photodiodes and red mud. *Hydrometallurgy* **2017**, *171*, 191–197. [CrossRef]
37. Davris, P.; Balomenos, E.; Panias, D.; Paspaliaris, I. Selective leaching ofrare earth elements frombauxite residue (redmud), using a functionalized hydrophobic ionic liquid. *Hydrometallurgy* **2016**, *164*, 125–135. [CrossRef]

38. Davris, P.; Balomenos, E.; Panias, D.; Paspaliaris, I. Chapter 12—Leaching Rare Earth Elements from Bauxite Residue Using Brønsted Acidic Ionic Liquids. In *Rare Earths Industry*; Elsevier: Amsterdam, The Netherlands, 2016; pp. 183–197.
39. Deng, B.; Li, G.; Luo, J.; Ye, Q.; Liu, M.; Rao, M.; Jiang, T.; Bauman, L.; Zhao, B. Selectively leaching the iron-removed bauxite residues with phosphoric acid for enrichment of rare earth elements. *Sep. Purif. Technol.* **2019**, *227*, 115714. [CrossRef]
40. Zhang, X.K.; Zhou, K.G.; Chen, W.; Lei, Q.Y.; Huang, Y.; Peng, C.H. Recovery of iron and rare earth elements from red mud through an acid leaching-stepwise extraction approach. *J. Cent. South Univ.* **2019**, *26*, 458–466. [CrossRef]
41. Zhao, F.P.; Yang, Z.Q.; Wei, Z.S. Polyethylenimine-modified chitosan materials for the recovery of La(III) from leachates of bauxiteresidue. *Chem. Eng. J.* **2020**, *388*, 124307. [CrossRef]
42. Yang, W.; Min, Z.; Yang, M.; Yan, J. Exploration of the Implementation of Carbon Neutralization in the Field of Natural Resources under the Background of Sustainable Development—An Overview. *Int. J. Environ. Res. Public Health* **2022**, *19*, 14109. [CrossRef]
43. Chen, T.; Guestrin, C. Xgboost: A scalable tree boosting system. In Proceedings of the 22nd Acm Sigkdd International Conference on Knowledge Discovery and Data Mining, San Francisco, CA, USA, 13–17 August 2016; pp. 785–794.
44. Jin, Z.; Zheng, M.; Liu, L.; Huang, Z.; Ye, L.; Wu, S.; Zeng, D.; Gu, J. Guizhou bauxite Distribution characteristics and enrichment mechanism of lithium in ore-bearing rocks [J/OL]. *Acta Geol. Sinica* **2022**, *1*, 225. [CrossRef]